

OMAE2008-57357

THE EFFECT OF A DUAL DRAFT HULL ON THE MOTION BEHAVIOUR OF A PIPELAY / HEAVY-LIFT VESSEL

J.L.F. van Kessel
GustoMSC,
Schiedam, The Netherlands

W.J. van der Velde
Seaway Heavy Lifting
Zoetermeer, The Netherlands

ABSTRACT

The motion behaviour of a Dual Draft vessel was calculated and experimentally validated by means of model tests. Both the tests and computations showed that the roll behaviour of a Dual Draft vessel in pipelay / transit mode does not correspond to the usual observed response amplitude operator (RAO), where the roll RAO decreases with increasing wave height due to non-linear damping. When the wider top section of the Dual Draft vessel enters the water due to a roll motion, the buoyancy increases at that side and results in an increase of the excitation moment and roll RAO.

Non-linear damping is of significant importance on the ship motions and is particularly noticeable in roll motions. This paper describes the effect of a Dual Draft hull on the motion behaviour of a pipelay / heavy-lift vessel in beam seas. The non-linear damping of a Dual Draft vessel will be discussed and calculations of the motion behaviour will be presented and compared with results of model tests.

KEYWORDS

Dual Draft vessel, pipelay vessel, heavy-lift vessel, motion behaviour, roll damping, roll statistics, model tests.

INTRODUCTION

The need for new and improved offshore pipelaying equipment is growing, since oil and gas discoveries are being made in deeper and rougher waters. In addition, many pipelay and heavy-lift vessels operating today were built during the seventies and eighties and will be replaced in the near future.

In recent years, pipelay functionality was added to several crane vessels. Besides, many contractors considering buying a new heavy-lift vessel are also interested in (future) pipelaying possibilities with the same vessel. In that case the vessel can be used for pipelay operations in periods with no (or few) heavy-lift assignments.

Design requirements with respect to stability and motion behaviour of a heavy-lift and a pipelay vessel are often conflicting. In general, metacentric heights (GM) of heavy-lift vessels are relatively high to provide sufficient stability for lifting operations, which are normally performed in calm weather conditions. On the other hand, pipelay operations will also be performed in more severe weather conditions.

Motions are for a large extent determined by the metacentric height of the vessel, which itself is to a large extent influenced by the breadth. A small breadth results in most cases in favourable motion behaviour. When a heavy-lift vessel is in lifting mode, the load in the crane will shift the centre of gravity upwards and decreases the GM-value. When not engaged in lifting operations but performing other functions, such as pipelaying or in transit, the motion behaviour of heavy-lift vessels is often unfavourable with high accelerations due to an excess in stability (GM height). In order to improve the motion behaviour of these types of vessels during pipelay operations, the metacentric height should be relatively low compared to the lifting mode.

For these reasons a Dual Draft hull was developed that combines a relatively large stability during heavy-lifting operations with good motion behaviour during transit and pipelay operations.

In addition the new developed hull shows good motion behaviour in pre-lifting mode when the vessel is at site and the crew is preparing the heavy-lift operation.

THE DUAL DRAFT VESSEL

The patented hull of a Dual Draft vessel comprises a narrow lower section from keel level to a widening level, and a top section with a larger width than the lower section extending from the widening level upwards toward deck level [7], as shown in Fig. 1.

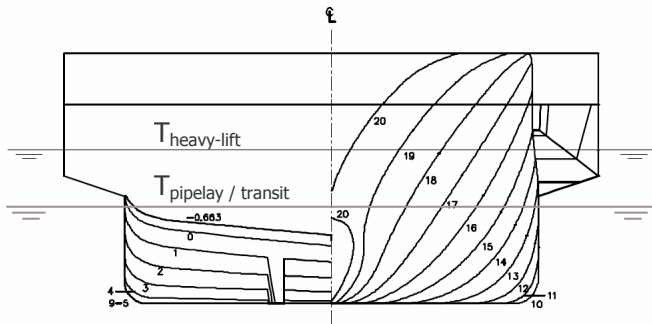


Figure 1: Body plan of the Dual Draft vessel

The vessel is ballasted to a relatively deep draft level in lifting mode such that the widening level is below water level. For pipelay and transit conditions the vessel is ballasted to a relatively shallow draft, in a way that the wide top section is above water level.

The sponsons start at the transom and run forward along the hull preferably between 50% and 90% of the length of the vessel. The sponsons have a simple rectangular form since they are only submerged during lifting operations. When submerged, they also contribute to a shift of the centre of buoyancy to the aft of the vessel.

Figure 2 shows the Dual Draft vessel in 3D. The hull design features a wave piercing bulbous bow and a slender fore ship which are both beneficial for transit speed. Compared to conventional pipelay / heavy-lift vessels, the resistance of the vessel is further reduced by ballasting to the shallow draft, resulting in a higher speed or more beneficial fuel consumption.

The aft ship was designed with a full form to offer sufficient buoyancy in lifting mode whilst still allowing for a good flow pattern to the propulsion thrusters. Due to the full aft ship and slender fore ship, the longitudinal centre of buoyancy (LCB) is located aft of the midship. Since the longitudinal centre of gravity (LCG) is also located aft of the midship, the amount of ballast water required for controlling the trim of the vessel is relatively small.

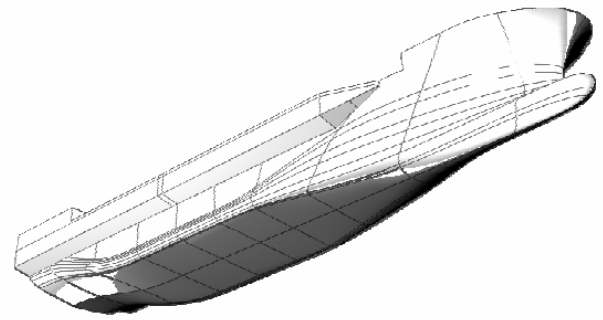


Figure 2: Dual Draft vessel

NUMERICAL APPROACH

This section briefly describes the main theory underlying the results of the next sections. Numerical calculations are performed with the linear 3-dimensional diffraction/radiation program AQWA-LINE. The floating structure is modelled in the usual way by means of panels representing pulsating sources distributed over the mean wetted surface of the vessel. The combinations of source strengths are calculated, which are required to diffract an incoming regular wave of given period, and to allow body oscillation in each degree of freedom.

The calm water wetted surface of the Dual Draft vessel is modelled by 3172 panels. In addition a lid was used to suppress the irregular frequencies which otherwise may occur. For non-linear time domain calculations the upper hull extending above the still water line is modelled by 2716 elements.

The source strengths laying in the centre of the panels are used to calculate the diffraction force, added mass and damping coefficients. Subsequently, the motions of the structure are determined by solving a six degree of freedom equation of motion taking into account the wave forces, added mass, damping and restoring terms.

The thus obtained diffraction force, added mass and damping coefficients are subsequently used by the time domain program AQWA-NAUT to calculate the wave frequency motions in irregular seas.

AQWA-NAUT calculates the hydrostatic forces and moments directly from the integral of hydrostatic pressure on all the elements which make up the submerged part of the body at each time step. The hydrostatic force on each element is given by:

$$\bar{F} = -\bar{n} \int_A p(x, y, z) dA \quad (1)$$

where:

$$\begin{aligned} p(x, y, z) &= -\rho g z \text{ for } z \leq 0, \text{ i.e. the hydrostatic pressure} \\ \bar{n} &= \text{the outward normal vector to the element} \\ A &= \text{the area of the element} \\ \rho &= \text{the density of water} \\ g &= \text{the acceleration due to gravity} \end{aligned}$$

The cut waterplane area together with the locations of the centre of buoyancy and the centre of gravity of the body determine the hydrostatic stiffness matrix. At each time step of the simulation the hydrostatic forces and moments are re-calculated based on the new submerged volume.

The Froude-Krylov wave forces are calculated at each time step by integrating the dynamic pressure acting on all submerged plate elements of the structure. The force on each element is calculated again by eq. (1), though this time p is the dynamic non-linear wave pressure for deep water [1]:

$$p(x, y, z) = \rho g \zeta \left(e^{kz} \cos(kx - \omega t) - \frac{1}{2} k \zeta e^{2kx} \right) \quad (2)$$

At each time step in the simulation, the position and velocity are known since they are calculated in the previous time step. From these, all position and velocity dependent forces, i.e. damping, mooring force, total wave force, drift force etc. are calculated. These are then summed to find the six total forces and moments for the structure. Next, the total force is equated to the product of the total mass (structural and added) and the rigid body accelerations.

The acceleration at the next time step can thus be determined. Forces are recomputed with the new position and velocity and the process is repeated to create the time history of motion. 20,000 time steps of 0.1 second are used to simulate the vessel motions in this contribution.

The model is kept in place by four soft-spring mooring lines in time domain calculation. Due to the large mass and soft-mooring system, the natural periods of oscillation in the horizontal degrees of freedom is in the order of minutes. At these periods there are no first order spectral energy so the system is not appreciably excited by first order forces in these degrees of freedom.

Though, AQWA-NAUT does not calculate low order drift forces, the structure can be excited by these forces as well.

Since the added mass/inertia and damping are not constant over the wave frequency range, these forces are modified to allow for this variation.

The total wave frequency force (i.e. diffraction plus Froude-Krylov) in each degree of freedom is calculated by the Cummins equation [8]:

$$\begin{aligned} [M + A(\infty)] \ddot{\zeta}(t) + B(\infty) \dot{\zeta}(t) + \\ \int_{-\infty}^t K(t-\tau) \dot{\zeta}(\tau) d\tau + C(t) \zeta(t) = F_{wf}(t) \end{aligned} \quad (3)$$

where:

$$\begin{aligned} A(\infty) &= \text{the Added mass coefficient at infinite frequency} \\ B(\infty) &= \text{the damping coefficient at infinite frequency} \\ C(t) &= \text{the matrix of hydrostatic restoring force coefficients, recalculated at each time step} \end{aligned}$$

The entries in the matrix $K(t-\tau)$ in the convolution integral are retardation functions of time, in which $\tau = t - dt$. When the retardation function is based on the damping only one single added mass entry should be known to obtain the whole added mass curve as described by Van Oortmerssen [8].

The matrix of hydrostatic restoring force coefficients and the wave force are re-calculated at every time step. The restoring coefficients significantly change when the wider top section enters the water. For this reason the stiffness matrix is non-linear and should be recalculated at every time step.

The total wave force in Eq. (3) is calculated and added to the sum of other forces to form the equation of wave frequency motions:

$$[m_s + m_d] \ddot{x}(t) = F_c(t) + F_w(t) + F_i(t) + F_h(t) + F_{wf}(t) \quad (4)$$

where:

$$\begin{aligned} \ddot{x} &= \text{the acceleration vector} \\ M &= \text{the structural mass} \\ A_d &= \text{the added mass and inertia at drift frequency} \\ [F_c] &= \text{the current forces} \\ [F_w] &= \text{the wind forces} \\ [F_i] &= \text{the mooring forces} \\ [F_h] &= \text{the hydrostatic forces} \\ [F_d] &= \text{the damping force} \end{aligned}$$

The total motion of the structure consists of a slow drift motion and a fast wave frequency position. The final position of the floating body in time-domain calculations is calculated by superposition of the 'slow' and 'wave frequency' positions.

MODEL TESTING

Model tests were performed to verify the numerical calculations and to establish the general seakeeping behaviour of the vessel.

Model tests were carried out in the Seakeeping and Manoeuvring basin at MARIN. The length, width and water depth of the basin are 170 x 40 x 5 m respectively. The basin is equipped with a flap type wave generator with 331 individual flaps of 0.4 m, each driven by an independent servo motor. This system facilitates the generation of regular waves and long crested or short-crested irregular waves in more or less arbitrary directions through the basin. A beach at the opposite side of the basin absorbs the incoming waves.

For the seakeeping tests a wooden model was built with a geometric scale of 1 to 36. The model was equipped with bilge keels and two azimuthing thrusters. Tests were performed for (pre-) hoisting and transit condition. The main particulars in full scale and for the model are given in Table 1.

Prior to the tests the longitudinal weight distribution of the model was determined on a low mass pendulum. The required longitudinal radius of inertia was obtained by fitting ballast at pre-calculated locations. The transverse weight distribution was adjusted in such a way that the natural period of roll matched the calculated natural period. The metacentric height was checked by means of a heeling test in calm water.

Table 1: Main particulars of the Dual Draft Vessel in pipelay and heavy-lift mode

Quantity	Symbol	Unit	Pipelay	Heavy-lift
Length between perpendiculars	L_{PP}	[m]	170.00	170.00
Breadth max	B	[m]	47.00	47.00
Breadth on waterline	B_{WL}	[m]	36.40	47.00
Draught	T	[m]	7.51	13.50
Draught on AP	T_A	[m]	7.51	13.51
Draught on FP	T_F	[m]	7.51	13.49
Displacement volume moulded	∇	[m ³]	33,358	70,977
Displacement mass in seawater	Δ	[t]	34,192	72,752
LCG position from APP	LCG	[m]	74.99	72.31
Transverse metacentric height	GM_T	[m]	4.20	11.70
Vertical position centre of gravity	KG	[m]	15.95	12.10
Mass radius of gyration around X-axis	K_{XX}	[m]	17.64	19.29
Mass radius of gyration around Y-axis	K_{YY}	[m]	55.40	46.44
Mass radius of gyration around Z-axis	K_{ZZ}	[m]	52.60	46.72
Natural period of roll	$T_{\phi n}$	[s]	19.30	12.06
Block coefficient	C_B	-	0.72	0.66
Length-Breadth ratio	L_{PP}/B	-	4.67	3.62
Breadth-Draught ratio	B/T	-	4.85	3.48

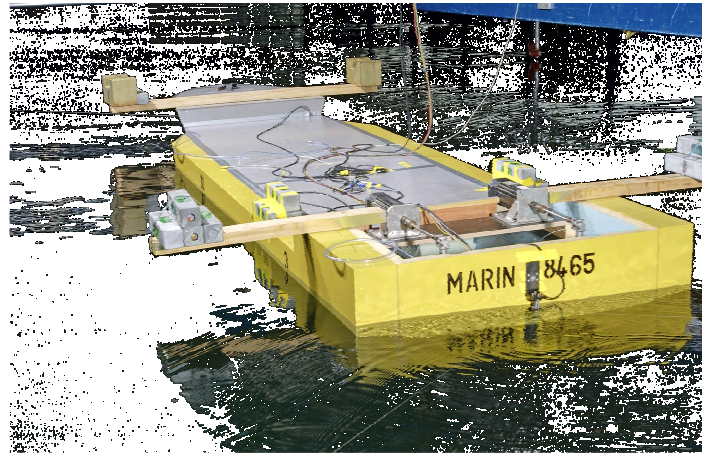


Figure 3: Scale model of the Dual Draft vessel being tested at deep (heavy-lift) draught

The program consisted of various tests in both the (pre-) hoisting condition and transit condition. In hoisting condition it was needed to bring ballast weights outside the model to meet the k_{yy} , GM and $T_{\phi n}$ requirements, as shown in Fig. 3.

In the transit condition the test program consisted of decay tests, tests at zero speed, tests for determining the current coefficients, and free sailing tests.

The model was moored fore and aft in an arrangement of soft springs during all zero speed tests and tests performed to determine the current coefficients. The natural frequency of the soft spring arrangement was selected such that first-order resonant response was avoided. The mooring lines are connected close to the free-water surface at an angle of 45 deg in the xy-plane at the bow and stern of the vessel.

All wave conditions were represented by JONSWAP spectra, which describe the wave energy distribution over the frequencies of young (growing) wind seas. A peak enhancement factor of 3.3 was used.

For sake of brevity, only results of the transit / pipelay condition in beam seas will be discussed in the remainder of this paper, as this condition clearly shows the effect of the unconventional hull on the motions of the vessel.

VISCOUS DAMPING

The influence of viscous damping on the roll motions of a vessel can be relatively large. An obvious source for viscous damping is the presence of appendages like bilge keels. Flow separation can also occur in absence of appendages, which is referred to as hull circulatory effects and adds viscous damping to the motion equation as well. Tanaka [6] determined these effects by means of model tests, while Ikeda et. al. [2-4] presented much research on roll damping in general.

Difficulties in predicting the roll damping of ships arise from its non-linear characteristics due to the effect of fluid viscosity. Besides, the forward speed of ships will also result in non-linear contributions.

Without viscous damping the motion equations are linear, i.e. the motion per unit wave amplitude (RAO) in each of the six degrees of freedom can be used to calculate the response in irregular seas. Consequently, the response in an irregular sea is the summation of the responses in regular waves, which define the spectrum.

The roll damping coefficient was derived from the decay test. Figure 4 shows the viscous part of the roll damping estimated as a function of the significant roll angle (dotted line). The viscous roll damping to be added is a function of the actual roll angle and depends on the actual sea-state.

The RAO's are calculated in AQWA using different percentages of added roll damping. With use of these RAO's the highest significant roll angle of a JONSWAP spectrum ($H_s = 4.5$ m, $T_p = 8.5$ sec, $\gamma = 3.3$) is calculated. The resulting significant roll angle as a function of added roll damping is shown in Fig. 4 (solid line). The intersection of the two lines gives the actual significant roll angle and the corresponding maximum viscous roll damping to be added.

In this case the added viscous damping is approximately 1.8% of the critical damping (b_{cr}), which can be expressed as:

$$b_{cr} = 2\sqrt{(M + A) \cdot C} \quad (5)$$

The thus obtained added damping is only valid for the maximum roll angles around the natural roll frequency. For smaller roll angles, at other frequencies, the viscous roll damping will be less than 1.8%.

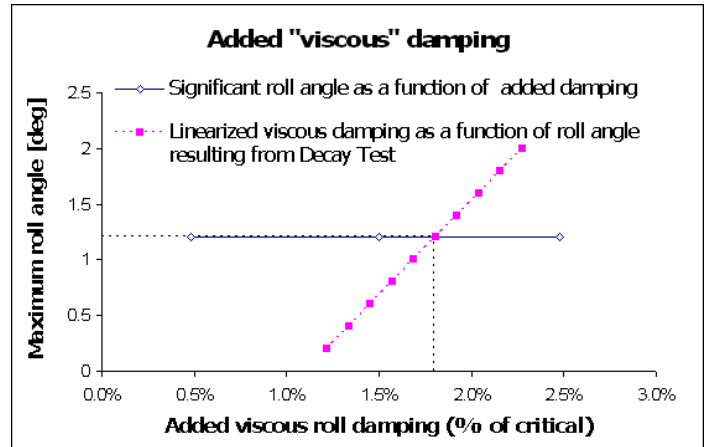


Figure 4: Added viscous damping

The wave energy spectrum and the heave RAO are presented in Fig. 5. This figure shows that maximum wave energy is located around the natural heave frequency.

Figure 6 shows the roll RAO in combination with the same wave energy spectrum. It can be seen that there is little energy in the waves around the natural roll frequency. Nevertheless this sea state with $T_p = 8.5$ sec. is chosen as it also clearly shows the effect of the dual draft hull on the roll motions of the vessel, this will be discussed in the next section.

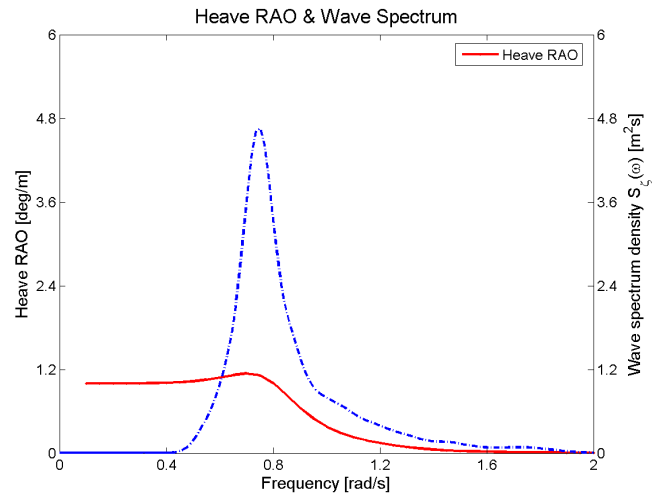


Figure 5: Heave responses in regular beam waves and energy density spectra for waves ($H_s = 4.5$ m, $T_p = 8.5$ sec. and $\gamma = 3.3$)

Figure 6 shows the RAO in which 1.8% of the critical damping is added to the potential damping according to Fig. 4.

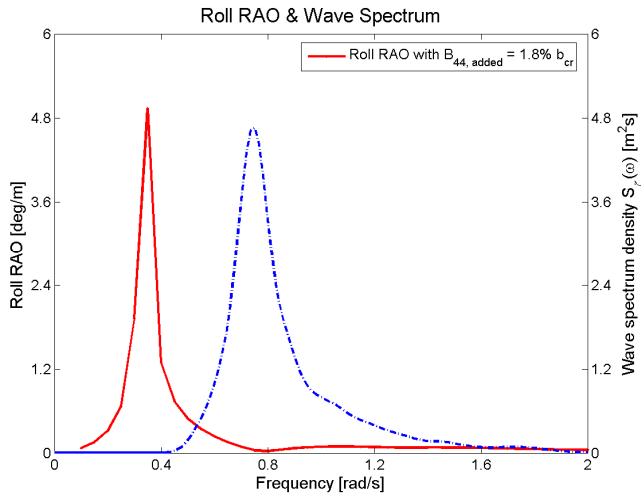


Figure 6: Roll responses in regular beam waves and energy density spectra for waves ($H_s = 4.5$ m, $T_p = 8.5$ sec. and $\gamma = 3.3$)

The roll RAO in regular beam waves can be used to estimate the viscous damping at smaller roll motions. The viscous roll damping at different frequencies can be estimated by:

$$B_{44,added}(\omega) = B_{44,added}(\omega_n) \frac{\left| \frac{z_a(\omega)}{z_a(\omega_n)} \right|}{\left| \frac{z_a(\omega)}{z_a(\omega_n)} \right| / \zeta_a(\omega_n)} \quad (6)$$

$$= B_{44,added}(\omega_n) \frac{\left| \frac{z_a(\omega)}{z_a(\omega_n)} \right|}{\left| \frac{z_a(\omega)}{z_a(\omega_n)} \right| / \zeta_a(\omega_n)}$$

Since $\zeta(\omega)$ and $\zeta(\omega_n)$ are equal in the linear frequency domain, Eq. (6) can be written as:

$$B_{44,added}(\omega) = B_{44,added}(\omega_n) \frac{RAO(\omega)}{RAO(\omega_n)} \quad (7)$$

Table 2 shows the viscous damping coefficients based on Eq. (7) at different wave frequencies for the sea state with a significant wave height of 4.5 m.

Table 2: Viscous damping at different frequencies in irregular seas ($H_s = 4.5$ m, $T_p = 8.5$ sec).

ω [rad/s]	Viscous damping	
	[t.m ² /s]	[% of b_{cr}]
0.35	1.55E+05	1.80%
0.5	1.54E+04	0.18%
0.95	2.80E+03	0.03%

The use of different viscous damping coefficients results in different roll RAOs as illustrated in Fig. 7. These RAOs (H) are obtained from the wave spectrum (S_ζ) and response spectrum (S_z) and can be calculated as follows:

$$S_z(\omega) = H^2 S_\zeta(\omega) \quad (8)$$

Figure 7 shows the results of experiments and non-linear calculations for roll motions in irregular seas in which $H_s = 4.5$ m, $T_p = 8.5$ sec. and $\gamma = 3.3$.

The use of Eq. (6) in estimating the viscous part of the roll damping shows good agreement with model tests at low and high frequencies. When the added damping is equal to 0.18% of the critical damping the measurements correspond well with the experiments at 0.50 rad/s. However, the computations tend to underestimate the results of model tests at frequencies between 0.75 and 1.05 rad/s. At higher frequencies the results of the computations are again close to those of model experiments, though roll responses are small.

Figure 7 shows the responses in the range from 0.5 to 1.1 rad/s since the wave energy is small outside this region.

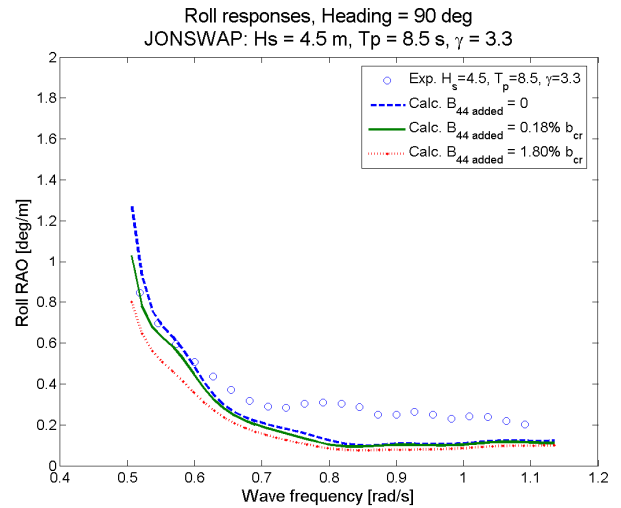


Figure 7: The effect of viscous roll damping on the roll RAOs

DISCUSSION OF MOTION BEHAVIOUR

Compared to existing pipelay / heavy-lift vessels, the unconventional hull shape and relatively low GM-value of a Dual Draft vessel will result in a different motion behaviour, especially at transit / pipelay mode.

First the motion behaviour of the Dual Draft vessel will be discussed based on responses in different sea states. The responses are normalized by dividing them by the wave amplitudes, which gives an 'average' impression of the motions in the frequency range.

Next, the motion behaviour will be discussed statistically and finally a short conclusion will be given.

Figure 8 shows the sway motions of the vessel in beam seas for different sea states in transit mode. An important variable in the sway motions of the vessel is the stiffness of the mooring system. A stiffness of 35 kN/m was used in the computations, resulting in a natural frequency of the mooring system (with vessel) which is approximately five times as small as the smallest natural frequency of the vessel. In this way the natural frequency of the mooring system will not influence the first order motions of the vessel.

Sway RAO's of the vessel should be approximately equal at different sea states since non-linear effects are small. Figure 8 confirms this and shows that the responses can be best predicted by linear diffraction calculations. Non-linear calculations tend to overestimate the experimental values at low and high frequencies.

Figure 9 shows that heave responses increase when the wider top section of the Dual Draft vessel enters the water. This effect is largest around the natural heave frequency of the vessel and is only visible in the results of the model tests. Non-linear calculations do not show a difference in heave response between different sea states.

At higher frequencies, results of experiments and computations are approximately equal and do not change with sea state. Results of linear calculations are slightly higher than those of non-linear computations around the natural frequency. Just like the sway motions, heave motions of the Dual Draft vessel can be well predicted by a linear approach.

Contrary, Fig. 10 clearly shows the non-linear behaviour of roll responses. In general, viscous roll damping increases when roll motions increase. The increase of viscous damping at large roll angles normally results in a decrease of roll RAOs.

However, roll RAOs of the Dual Draft vessel increase when the sea state increases due to an unconventional hull. The excitation moment on the body significantly increases when the wider top section of the hull enters the water at one side. This moment is highly non-linear in case of a Dual Draft hull resulting in large roll RAO's at high sea states.

Results of non-linear computations show good agreement for the two highest sea states at low frequencies. However, the computations tend to underestimate the results of model tests at frequencies between 0.75 and 1.05 rad/s as discussed in the previous section. In addition, roll responses are small at low sea states and high frequencies, by which it is difficult to predict them accurately.

Since the influence of non-linear effects is small at the lowest sea state, the results of linear and non-linear computations are approximately equal for this condition.

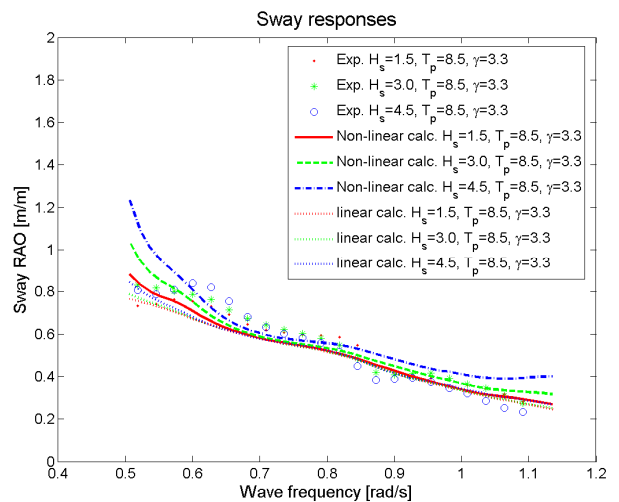


Figure 8: Sway RAOs at different sea states

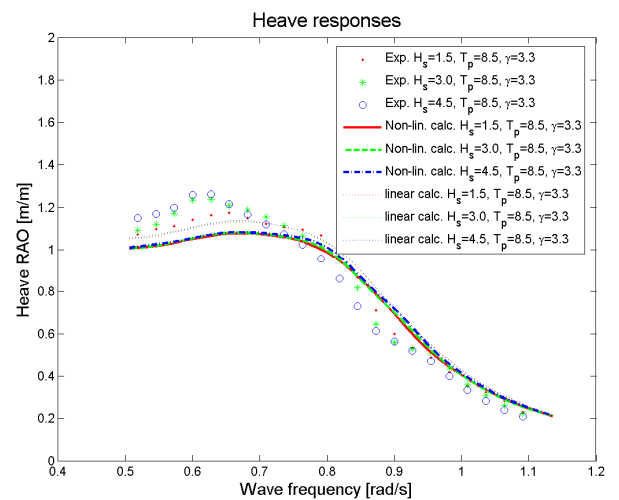


Figure 9: Heave RAOs at different sea states

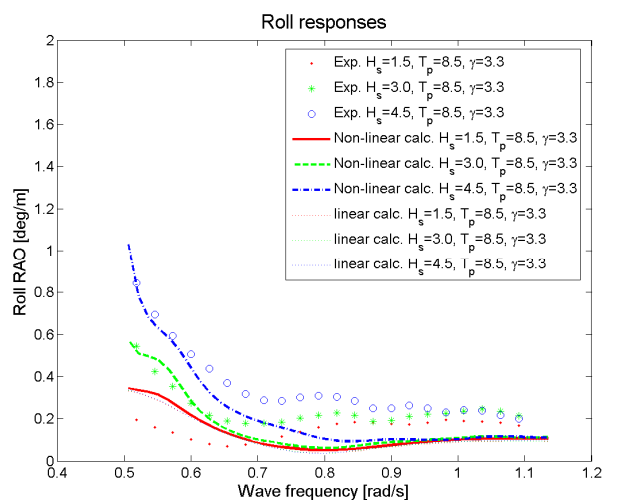


Figure 10: Roll RAOs at different sea states

The amount of added damping in Fig. 8-10 is 0.18% of the critical damping as discussed in the previous section. Consequently, the results of the linear computations in Fig. 10 are (approximately) equal to those of the linear frequency domain in Fig. 6.

Hitherto, the discussion of the motion behaviour of the Dual Draft vessel was based on responses in different sea states. Responses were normalized by dividing them by the wave amplitudes, which gives an 'average' impression of the motions in the frequency range.

In addition, motions of the Dual Draft vessel are also analyzed statistically. Such an approach will provide a better understanding of the distribution of the wave amplitudes over time.

In this case the extremes of the complete time-domain simulations are analyzed. For this reason it is necessary to add 1.8% of the critical damping to the linear (potential) damping coefficients as discussed in the previous section. Since the wave spectrum is narrow banded and wave amplitudes satisfy a Gaussian distribution around zero, wave statistics can be approximated by a Rayleigh distribution as described by Journee [5]:

$$f(x|\sigma) = \frac{x}{\sigma^2} \exp\left(\frac{-x^2}{2\sigma^2}\right) \quad (9)$$

in which x is the wave amplitude and σ its standard deviation.

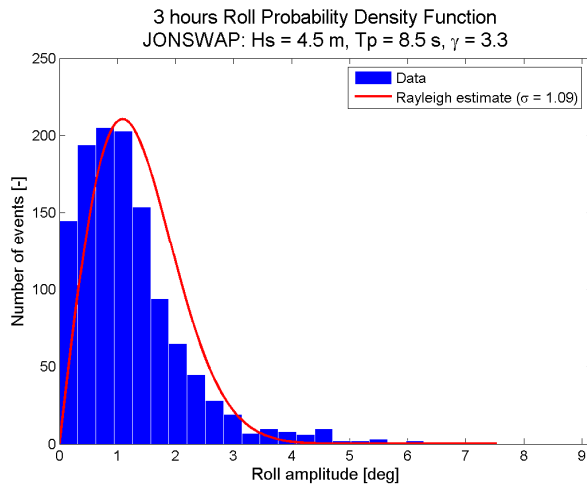


Figure 11: Rayleigh Probability Density Function of number of roll amplitudes in irregular beam sea

As the roll spectrum is also narrow banded, Eq. (9) holds for the roll motions as well. Figure 11 shows the Rayleigh probability density function of the roll amplitudes in

irregular beam seas of 4.5 m significant wave height. When the results of time domain calculations are compared with the Rayleigh estimate, it is clear that the Rayleigh approach underestimates the number of low and high roll amplitudes, see Fig. 11. This figure shows the maximum roll amplitudes occurring in time-domain simulations of 3 hours.

A Rayleigh probability density function can be derived from the Eq. (9). The probability that the roll amplitude (X_{4a}) exceeds a chosen threshold value (a) can be expressed as:

$$P(X_{4a} > a) = \int_a^\infty f(x|\sigma) dx = \exp\left(\frac{-a^2}{2\sigma^2}\right) \quad (10)$$

Figure 12 shows the probability of exceedance in beam seas of 4.5 m significant wave height. Both results of time-domain calculations and the Rayleigh estimate are plotted in the same figure. A conventional hull, with constant beam from keel to deck level, would follow the Rayleigh estimate as plotted in Fig. 12.

The figure clearly shows the effect of the wider top section of the Dual Draft vessel on the roll amplitudes; Rayleigh overestimates the probability of exceedance at small wave amplitudes and underestimates it at large wave amplitudes.

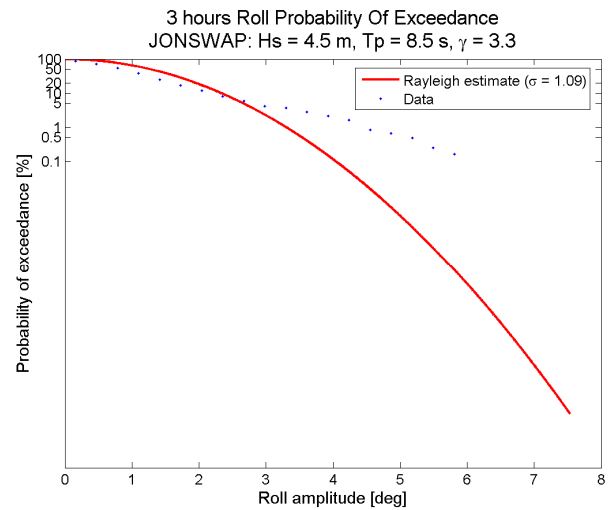


Figure 12: Probability of exceeding of roll amplitudes in irregular beam seas

In less severe seas when waves do not hit the wider top section of the Dual Draft vessel and the restoring coefficients are constant over time, roll amplitudes correspond to those of the Rayleigh estimate, i.e. the wider top section has no effect on the roll motion and the

motion behaviour is similar to that of a conventional vessel.

Figure 13 shows the probability of exceedance of the roll motions in beam seas with a significant wave height of 1.5 m.

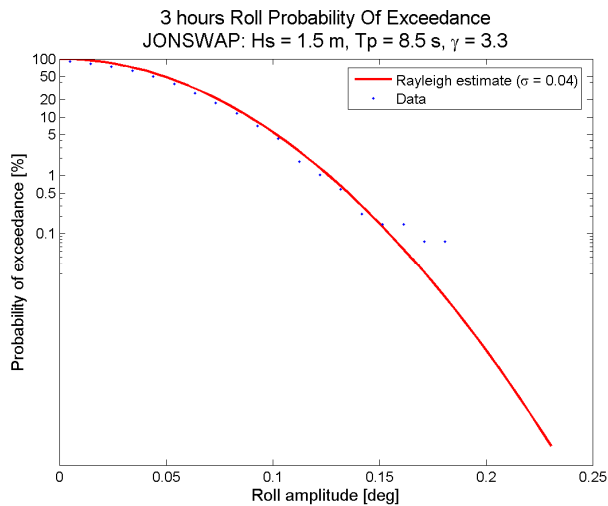


Figure 13: Probability of exceeding of roll amplitudes in irregular beam sea

Finally it should be noted that the relatively small waterline beam of the Dual Draft vessel at pipelay / transit mode significantly lowers the GM-value as discussed in the first section of this paper. As a result the overall motion behaviour of a heavy-lift / pipelay vessel will improve compared to a conventional hull.

CONCLUSIONS

The motion behaviour of a Dual Draft vessel was calculated and experimentally validated by means of model tests. Both tests and computations showed that the roll behaviour of a Dual Draft vessel in pipelay / transit mode does not correspond to the usual observed response amplitude operator (RAO), where the roll RAO decreases with increasing wave height due to non-linear damping. When the wider top section of the Dual Draft vessel enters the water due to a roll motion, the buoyancy increases at that side and results in an increase of the excitation moment and roll RAO.

On the other hand, the excess in stability typically for these types of vessels is significantly reduced due to the relatively small water line area in pipelay / transit mode. The reduced GM-value results in an improved motion behaviour of pipelay / heavy-lift vessels in general.

Finally, the overall motion behaviour of a heavy-lift / pipelay vessel will improve when the vessel is designed with a dual draft hull.

REFERENCES

1. AQWA-NAUT manual, *Century Dynamics* Limited, 2006.
2. Ikeda, Y., Himeno, Y. and Tanaka, N. *On roll damping force of ship - effect of hull surface pressure created by bilge keels*. Journal of Society of Naval Architects of Japan, 1979 No. 165, pp.41-49.
3. Ikeda, Y., Himeno, Y. and Tanaka, N., *On eddy making component of roll damping force on naked hull*. Journal of Society of Naval Architects of Japan, 1977, No.142, pp. pp.59-69.
4. Ikeda, Y., Ishikawa, M. and Tanaka, N. *Viscous effect on damping forces of ship in sway and roll coupling motion*. Journal of the Kansai Society of Naval Architects, Japan, 1981, No.180, pp.69-75.
5. Journee, J.M.J. and Massie, W.M., *Offshore hydrodynamics*. Delft University of Technology, 2001.
6. Tanaka, N., Himeno, Y. and Ikeda, Y. *Comparison of roll damping between prediction and measurement*. Osaka University, Department of Naval Architecture, Presented at the ITTC Seakeeping Committee, March 1980.
7. Van Der Velde, W.J., Wassink, W.J.A. and Commandeur, J.A. *Dual draft vessel*, Int. Patent, publication number: WO/2007/069897, 2007.
8. Van Oortmerssen, G. *The motions of a moored ship in waves*. PhD thesis, Delft Univ. of Technology, Delft, The Netherlands, 1976.